Available online at www.worldscientificnews.com

World Scientific News

An International Scientific Journal

WSN 140 (2020) 59-78 EISSN 2392-2192

Homotopy Perturbation Method of Hydromagnetic Flow and Heat Transfer of a Casson Fluid over an Exponentially Shrinking Sheet

Thiagarajan Murugesan[1], **S. Varshini**[2] and **M. Dinesh Kumar**[3]

Department of Mathematics, PSG College of Arts & Science, Coimbatore, India

[1-3]E-mail address: thiyagu2665@gmail.com , svarshini0808@gmail.com , dineshmdkc.111@gmail.com

ABSTRACT

Nonlinear hydromagnetic flow and heat transfer of a Casson fluid over an exponentially shrinking sheet has been investigated. The fluid is assumed to be viscous, incompressible and electrically conducting. The similarity transformations are applied to reduce the non-linear partial differential equations into the non-linear ordinary differential equations. Homotopy Perturbation Method is used to solve the resulting non-linear differential equations under appropriate boundary conditions. The impact of Casson fluid parameter, magnetic interaction parameter, suction parameter and Prandtl number on both velocity and temperature profiles are shown graphically. Thermal boundary layer thickness decreases with increasing Prandtl number. Effect of Casson fluid parameter is to reduce both the velocity and temperature. Quantities of physical interest such as skin-friction coefficient, non-dimensional rate of heat transfer are solved numerically. A comparison reveals a remarkable agreement between the Homotopy Perturbation Method and Runge-Kutta fourth order method.

***Keywords*:** MHD, Casson Fluid, suction, Homotopy Perturbation method, Runge-Kutta method

(Received 12 December 2019; Accepted 31 December 2019; Date of Publication 02 January 2020)

1. INTRODUCTION

The MHD Boundary layer flow over the shrinking surface is being investigated in several technological processes, since the magnetic field on viscous flow of electrically conducting fluid in the industrial process namely manufacturing of glass sheets, purification of crude oil, magnetohydrodynamic electrical power generation and many more. The study on the boundary layer flow of a viscous fluid towards a linear stretching sheet was first initiated by Crane [1, 2]. Further, Crane and Carragher [3] examined heat transfer on continuous stretching sheet. From then, many researchers examined the flow over a stretching or shrinking sheet under different aspects of MHD, heat and mass transfer and several other phenomena. Salem [4] discussed the effects of variable properties on MHD heat and mass transfer flow near the stagnation point towards a stretching sheet in a porous medium with thermal radiation. Bhattacharyya [5] analysed the slip effects on diffusion of flow over a vertical stretching sheet with suction and blowing, also the slip effects on an unsteady boundary layer stagnation point flow and heat and mass transfer towards a stretching sheet.

In recent trends, researchers have studied on shrinking sheet. In the shrinking sheet the velocity on the boundary is towards a fixed point. The shrinking sheet is not confined within a boundary layer, and the flow exists unless an adequate suction on the boundary is imposed. Many researchers have started investigating the shrinking sheet boundary layer flow problem due to its wide range of applications. For example, the shrinking film is used in packaging bulk products. In addition, suction occurs when the fluid condenses on the surface as in chemical vapour deposition.

Wang [6] initiated the flow over a shrinking sheet is distinct comparatively to the stretching sheet flow since the effect of shrinking, the generated vorticity does not remain inside the boundary layer. Later, Miklavcic and Wang [7] established the study of viscous flow due to a shrinking sheet to study the properties of the flow due to the shrinking sheet with suction. Fang [8, 9] discussed the magnetohydrodynamic viscous flow of Newtonian fluid over a shrinking sheet with wall mass transfer taking the slip as well as the no-slip boundary conditions. Hayat [10] studied the three-dimensional rotating flow induced by the shrinking sheet for suction. Recently, Jhankal et al. [11] studied the MHD boundary layer flow past a shrinking sheet with heat transfer and mass suction.

The Casson fluid is one among the type of non-Newtonian fluids which exhibits yield stress. Casson fluid is defined as the shear thinning liquid that has infinite viscosity at zero rate of stress, a yield stress below which no flow occurs and a zero viscosity at an infinite rate of shear. That is, if a shear stress lesser than the yield stress is applied to the fluid, it behaves like solid. On the other hand, a shear stress greater than the yield stress when applied to the fluid, it moves. Human blood is considered as the Casson fluid due to the presence of the substances like protein, fibrinogen in the aqueous plasma, the red blood cells form a chainlike structure known as aggregates or rouleaux. Jelly, honey and concentrated juices are some of the examples of Casson fluid by Pramanik [12].

In the recent years, many researchers have studied the semi analytical solution of real life mathematical modelling which are nonlinear differential equations with variable coefficients. More than numerical methods, semi analytical methods are applied to the solution of nonlinear non-homogeneous partial differential equations by He et al. [13-17]. One of the most powerful semi analytical method to solve non-homogeneous partial differential equations is the Homotopy Perturbation Method (HPM). He [1] developed the homotopy perturbation method

to solve linear, nonlinear, initial and boundary value problems by combining the standard homotopy and Perturbation Technique. Ganji et al. [18] studied the application of He's Homotopy Perturbation Method to nonlinear coupled systems of reaction-diffusion equations. Nourazer et al. [19] investigated MHD Nanofluid flow over a horizontal stretching plate by HPM. Recently, Thiagarajan and Senthil Kumar [20] analysed the differential transform method-Pade approximation of MHD boundary layer flow of a Casson fluid over a shrinking sheet. Upto the authors knowledge, no one has attempted MHD flow and heat transfer of a Casson fluid over a shrinking sheet using HPM.

In this paper, viscous, incompressible hydromagnetic boundary layer flow and heat transfer of a Casson fluid over a shrinking sheet by homotopy perturbation method is studied. The governing equations of this problem are non-linear partial differential equations which are then reduced to non-linear ordinary differential equations using similarity transformation. Using homotopy perturbation method, the boundary value problem is converted into an initial value problem. The consequences of non-dimensional governing parameters namely Casson fluid parameter, magnetic interaction parameter, Prandtl number and suction parameter on velocity, temperature, skin friction and rate of heat transfer are presented graphically and thoroughly discussed.

2. MATHEMATICAL FORMULATION

Consider a two-dimensional flow of an incompressible Casson fluid over an exponentially shrinking sheet. By variable magnetic field applied normal to the field, the fluid becomes electrically conducting whereas the induced magnetic field is neglected under the approximation of small Reynold's number. Figure 1 represents the configuration of the shrinking sheet.

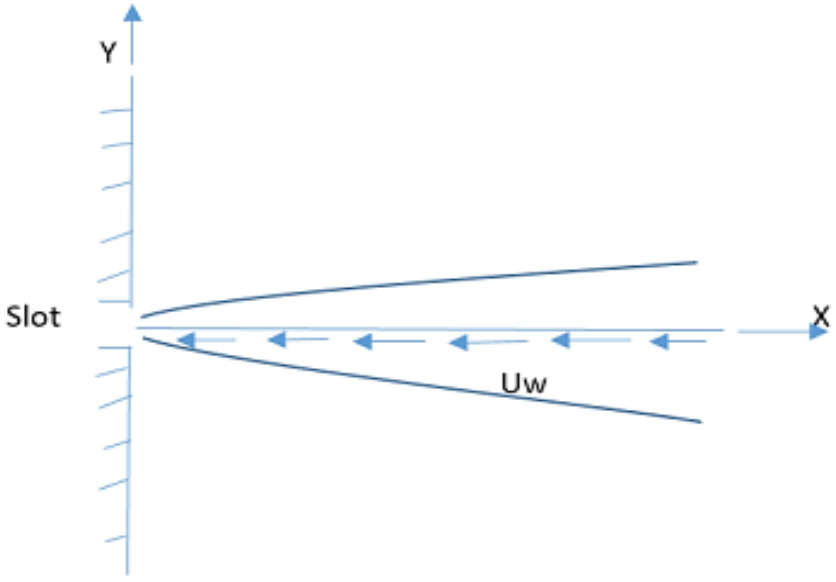

Figure 1. Shrinking Sheet Configuration

Suppose the equation of Casson fluid, reported by Mustafa [21] is given by,

$$\tau^{1/n} = \tau_0^{1/n} + \mu\gamma^{1/n} \tag{1}$$

(or)

$$\tau_{ij} = \left[\mu_B + \left(\frac{P_y}{\sqrt{2\pi}} \right)^{1/n} \right]^n 2e_{ij} \tag{2}$$

where μ is the dynamic viscosity, μ_B is the plastic dynamic viscosity of the non-Newtonian fluid, P_y is the yield stress of the fluid, π is the product of the component of deformation rate with itself namely, $\pi = e_{ij} e_{ij}$ and e_{ij} is the (i, j)th component of deformation rate.

The governing equations of the problem involving equations of motion, momentum and energy equations governing such type of flow is given by

$$\frac{\partial u}{\partial x} + \frac{\partial v}{\partial y} = 0 \tag{3}$$

$$u\frac{\partial u}{\partial x} + v\frac{\partial u}{\partial y} = \nu\left(1 + \frac{1}{\gamma}\right)\frac{\partial^2 u}{\partial y^2} - \frac{\sigma B^2}{\rho}u \tag{4}$$

$$u\frac{\partial T}{\partial x} + v\frac{\partial T}{\partial y} = \alpha\frac{\partial^2 T}{\partial y^2} \tag{5}$$

The boundary conditions are

$$u = U_w(x) = -U_0 \exp\left(\frac{x}{l}\right) \text{ at y = 0} \tag{6}$$

$$v = V_w(x) = V_0 \exp\left(\frac{x}{2l}\right) \quad \text{at y=0, } T = T_w \text{ at y = 0}$$

$$u \to 0 \text{ as } y \to \infty, T \to T_\infty \text{ as } y \to \infty \tag{7}$$

In the boundary conditions above, U_w is the shrinking velocity with U_0 being a shrinking constant and V_w is the mass transfer velocity with $V_0 > 0$ for mass suction, u and v are components of velocity in the x and y directions respectively, T is the temperature,

$\alpha = \dfrac{\kappa}{(\rho C_p)}$ is the ratio of thermal conductivity to the product of density and specific heat of the fluid, l is the characteristic length and *B(x)* being the magnetic field which is of the form

$$B = B_0 \exp\left(\frac{x}{2l}\right)$$

where B_0 is the constant magnetic field. The stream functions are introduced and are being defined as follows

$$u = \frac{\partial \psi}{\partial y}, \quad v = -\frac{\partial \psi}{\partial x} \tag{8}$$

The similarity transformations are given by,

$$\psi = \sqrt{2\nu l U_0}\, f(\eta) \exp\left(\frac{x}{2l}\right) \tag{9}$$

$$\eta = y\sqrt{\frac{U_0}{2\nu l}} \exp\left(\frac{x}{2l}\right)$$

$$\theta(\eta) = \frac{T - T_\infty}{T_w - T_\infty}$$

where η is the independent similarity variable and T_∞ is the free stream temperature. Using the above similarity transformations, equation of continuity is identically satisfied and the momentum equation takes the form

$$\left(1 + \frac{1}{\gamma}\right) f''' - Mf' + ff'' - 2(f')^2 = 0 \tag{10}$$

$$\theta'' + \Pr f\theta' = 0 \tag{11}$$

The corresponding boundary conditions are

$$f = s,\ f' = -1 \text{ at } \eta = 0 \tag{12}$$

$$f' \to 0 \text{ as } \eta \to \infty$$

$$\theta = 1 \text{ at } \eta = 0,\ \ \theta = 0 \text{ as } \eta \to \infty$$

where

γ = Casson fluid parameter, $M = \frac{2\sigma B^2 l}{\rho U_0}$ is the magnetic interaction parameter, $\Pr = \frac{\nu}{\alpha}$ is the Prandtl number and $s = \frac{-V_w}{\sqrt{\frac{\nu U_0}{2l}}} > 0$ is the suction parameter.

The physical quantities are the skin-friction coefficient C_f and the local Nusselt number Nu_x which are being defined as

$$C_f = \frac{\tau_w}{\rho U_w^2(x)} \quad \text{and} \quad Nu_x = \frac{xq_w}{k(T_w - T_\infty)} \tag{13}$$

where τ_w being the skin friction along the sheet and q_w being the heat flux from the surface. Using the similarity variables, it gives

$$\mathrm{Re}_x^{1/2} C_f = \left(1 + \frac{1}{\gamma}\right) f''(0) \quad \text{and} \quad \frac{Nu_x}{\mathrm{Re}_x^{1/2}} = -\theta'(0) \tag{14}$$

where $\mathrm{Re}_x = \frac{U_w x}{\nu e^{-x/l}}$ is the local Reynolds number.

3. HOMOTOPY PERTURBATION METHOD

Homotopy Perturbation Method proposed by He [1], Consider the non-linear differential equations:

$$L(u)+N(u) = f(r),\ r \in \Omega \tag{15}$$

with boundary condition

$$B\left(u, \frac{\partial u}{\partial n}\right) = 0,\ r \in \Omega \tag{16}$$

where L is defined as the linear differential operator, N being the non-linear operator, f(r) is the analytic function, B is the boundary operator and Γ is the boundary of the domain Ω. Thus we obtain the equation

$$L(u)+N(u)-f(r)=0,\ r \in \Omega \tag{17}$$

We construct the homotopy of the form

$$\nu(r, p) : \Omega \times [0,1] \to R$$

which satisfies

$$H(v,p) = (1-p)[L(v) - L(u_0)] + p[A(v) - f(r)] = 0 \tag{18}$$

$$p \in [0,1], r \in \Omega \tag{19}$$

where $p \in [0,1]$ is an embedding parameter and u_0 is an initial approximation which satisfies the boundary conditions.

Thus we have:

$$H(v,0) = L(v) - L(u_0) = 0$$
$$H(v,1) = A(v) - f(r) = 0$$

The changing process of p from 0 to 1 is just that of $v(r,p)$ from u(r) is said to be a deformation. $L(v) - L(u_0)$ and $A(v) - f(r)$ are called homotopy. According to the HPM, assuming the embedding parameter to be small, also equations can be written in the form of power series as

$$v = v_0 + pv_1 + p^2 v_2 + \ldots$$

Setting p = 1, the results are as follows

$$u = \lim_{p \to 1} v = v_0 + v_1 + v_2 + \ldots \tag{20}$$

Equating the power series of p we obtain,

$$p^0 : L(v_0) = L(u_0)$$
$$p^1 : L(v_1) = h_1 u_0 - f(r)$$
$$p^2 : L(v_2) = h_1(u_0, u_1)$$
$$p^3 : L(v_3) = h_1(u_0, u_1, u_2)$$
$$\vdots$$

and so on. Where $u_1, u_2, u_3 \ldots$ are the functions that satisfies the following equation

$$h(u_0 + pu_1 + p^2 u_2 + \ldots) = h_1(u_0) + ph_2(u_0, u_1) + p^2 h_3(u_0, u_1, u_2) + \ldots \tag{21}$$

The initial function u_0 is splitted into two parts as follows

$$u_0 = H_0 + H_1$$

The above form is used instead of the iteration procedure, we get the solution by homotopy perturbation method that depends on the choice of H_0 and H_1.

4. SOLUTION OF THE PROBLEM

Using the homotopy perturbation method the equations are rewritten as follows

$$(1-p)\left[\left(1+\frac{1}{\gamma}\right)f'''-\left(1+\frac{1}{\gamma}\right)f_0'''\right]+p\left[\left(1+\frac{1}{\gamma}\right)f'''-M\quad f'+ff''-2(f')^2\right]=0 \tag{22}$$

$$(1-p)[\theta''-\theta_0'']+p[\theta''+\Pr\ f\theta']=0 \tag{23}$$

The power series of the homotopy parameter p with the approximation of f and θ are as follows

$$\begin{aligned} f &= f_0+pf_1+p^2f_2+\ldots=\sum_{i=1}^{n}p^i f_i \\ \theta &= \theta_0+p\theta_1+p^2\theta_2+\ldots=\sum_{i=1}^{n}p^i\theta_i \end{aligned} \tag{24}$$

The terms independent of p is given by

$$\begin{aligned} f_0'''&=0 \\ \theta_0''&=0 \end{aligned} \tag{25}$$

The boundary conditions are

$$f_0(0)=s;\ f_0'(0)=-1;\ f_0'(\infty)=0;\quad \theta_0(0)=1;\theta_0(\infty)=0 \tag{26}$$

The terms containing the p terms are as follows

$$\left(1+\frac{1}{\gamma}\right)f_1'''+\left(1+\frac{1}{\gamma}\right)f_0'''-Mf_0'+f_0f_0''-2(f_0')^2=0 \tag{27}$$

$$\theta_1''+\theta_0''+\Pr\ f_0\theta_0'=0 \tag{28}$$

The boundary conditions are

$$f_1(0)=0;\ f_1'(0)=0;\ f_1'(\infty)=0;\quad \theta_1(0)=0;\theta_1(\infty)=0 \tag{29}$$

The coefficient of p^2 terms are as follows

$$\left(1+\frac{1}{\gamma}\right)f_2'''-Mf_1'+f_0f_1''+f_1f_0''-2f_0'f_1'=0 \tag{30}$$

$$\theta_2''+\Pr(f_0\theta_1'+f_1\theta_0')=0 \tag{31}$$

The boundary conditions being

$$f_2(0)=0;\ f_2'(0)=0;\ f_2'(\infty)=0;\quad \theta_2(0)=0;\theta_2(\infty)=0 \tag{32}$$

Solving the above equations with their corresponding boundary conditions using maple we would obtain

$$f_0=\frac{1}{10}\eta^2-\eta+s \tag{33}$$

$$\begin{aligned} f_1=&\frac{\gamma}{50(\gamma+1)}\left[\frac{5}{12}M\eta^4-\frac{25}{3}M\eta^3+\frac{1}{20}\eta^5-\frac{5}{4}\eta^4-\frac{5}{3}s\eta^3+\frac{50}{3}\eta^3\right]\\ &+\frac{\gamma}{48(\gamma+1)}(40M+12s-75)\eta^2 \end{aligned} \tag{34}$$

$$\begin{aligned} f_2=&\frac{\gamma^2}{15000(\gamma+1)^2}\left(\frac{25}{6}M^2\eta^6-125M^2\eta^5+\frac{10}{7}M\eta^7+\frac{3125}{3}M^2\eta^4\right)\\ &+\frac{\gamma^2}{15000(\gamma+1)^2}\left(-50M\ \eta^6-50M\ \eta^5 s+\frac{9}{112}\eta^8+750M\ \eta^5+\frac{1875}{2}M\eta^4 s\right)\\ &+\frac{\gamma^2}{15000(\gamma+1)^2}\left(-\frac{45}{14}\eta^7-\frac{55}{6}s\eta^6-\frac{40625}{8}M\ \eta^4-\frac{12500}{3}M\eta^3 s+\frac{475}{6}\eta^6\right)\\ &+\frac{\gamma^2}{15000(\gamma+1)^2}\left(200s\eta^5+125\eta^4 s^2-\frac{3875}{4}\eta^5-\frac{4375}{2}s\eta^4-1250\eta^3 s^2\right)\\ &+\frac{\gamma^2}{15000(\gamma+1)^2}\left(\frac{46875}{8}\eta^4+\frac{15625}{2}s\eta^3\right)\\ &-\frac{5\gamma^2}{4032(\gamma^2+2\gamma+1)}\left(1120M^2-5250M\ -168s^2-294s+5835\right)\eta^2 \end{aligned} \tag{35}$$

$$\theta_0=-\frac{\eta}{5}+1 \tag{36}$$

$$\theta_1=\frac{\Pr}{50}\left(\frac{1}{12}\eta^4-\frac{5}{3}\eta^3+5s\eta^2\right)+\left(-\frac{1}{2}\Pr s+\frac{5}{8}\Pr\eta\right) \tag{37}$$

$$\theta_2 = \frac{\Pr}{30000(\gamma+1)}(-2500\gamma\,\Pr\eta^3 s - 9375\gamma\,\Pr\eta^2 s + 875\gamma\,\Pr\eta^4 s + 7500\Pr\eta^2\gamma s^2)$$
$$+\frac{\Pr}{30000(\gamma+1)}\left(-40\gamma\,\Pr\eta^5 s - 1000\Pr\eta^3\gamma s^2 - 50M\eta^5\gamma + \frac{50}{3}\gamma\,\Pr\eta^6\right)$$
$$+\frac{\Pr}{30000(\gamma+1)}\left(-150\eta^5\,\Pr + 100\eta^5\gamma - \frac{3125}{4}\eta^4\gamma + 875\eta^4\,\Pr s\right)$$
$$+\frac{\Pr}{30000(\gamma+1)}\left(125\eta^4\gamma s + 7500\Pr s^2\eta^2 + \frac{5}{3}M\eta^6\gamma - \frac{10}{21}\gamma\,\Pr\eta^7\right)$$
$$+\frac{\Pr}{30000(\gamma+1)}\left(-40\eta^5\,\Pr s - 10\eta^5\gamma s - 1000\Pr s^2\eta^3 + \frac{1250}{3}M\ \eta^4\gamma\right)$$
$$+\frac{\Pr}{30000(\gamma+1)}\left(-2500\eta^3\,\Pr s - 9375\eta^2\,\Pr s - \frac{625}{4}\Pr\eta^4 + 3125\Pr\eta^3\right)$$
$$+\frac{\Pr}{30000(\gamma+1)}\left(\frac{50}{3}\eta^6\,\Pr - \frac{10}{21}\eta^7\,\Pr + \frac{1}{7}\eta^7\gamma - 5\eta^6\gamma\right)$$
$$-\frac{5\Pr\eta}{4032(\gamma+1)}(336\Pr\gamma s^2 + 700M^2\gamma - 672\Pr\gamma s + 336\Pr s^2 + 255\gamma\,\Pr)$$
$$-\frac{5\Pr\eta}{4032(\gamma+1)}(-672\Pr s + 252s\gamma + 255\Pr - 1305\gamma) \qquad (38)$$

In general the values of f and θ are obtained by simplifying

$$f = f_0 + pf_1 + p^2 f_2 + \ldots$$
$$\theta = \theta_0 + p\theta_1 + p^2\theta_2 + \ldots \qquad (39)$$

$$f = \frac{1}{10}\eta^2 - \eta + s + \frac{\gamma}{50(\gamma+1)}\left[\frac{5}{12}M\eta^4 - \frac{25}{3}M^2\eta^3 + \frac{1}{20}\eta^5 - \frac{5}{4}\eta^4 - \frac{5}{3}s\eta^3 + \frac{50}{3}\eta^3\right]$$
$$+\frac{\gamma^2}{15000(\gamma+1)^2}\left(\frac{25}{6}M^2\eta^6 - 125M^2\eta^5 + \frac{10}{7}M\eta^7 + \frac{3125}{3}M^2\eta^4\right)$$
$$+\frac{\gamma^2}{15000(\gamma+1)^2}\left(-50M\eta^6 - 50M\eta^5 s + \frac{9}{112}\eta^8 + 750M\eta^5 + \frac{1875}{2}M\eta^4 s\right)$$
$$+\frac{\gamma^2}{15000(\gamma+1)^2}\left(-\frac{45}{14}\eta^7 - \frac{55}{6}s\eta^6 - \frac{40625}{8}M\eta^4 - \frac{12500}{3}M\eta^3 s + \frac{475}{6}\eta^6\right) \qquad (40)$$
$$+\frac{\gamma^2}{15000(\gamma+1)^2}\left(200s\eta^5 + 125\eta^4 s^2 - \frac{3875}{4}\eta^5 - \frac{4375}{2}s\eta^4 - 1250\eta^3 s^2\right)$$
$$+\frac{\gamma^2}{15000(\gamma+1)^2}\left(\frac{46875}{8}\eta^4 + \frac{15625}{2}s\eta^3\right)$$
$$-\frac{5\gamma^2}{4032(\gamma^2+2\gamma+1)}\left(1120M^2 - 5250M\ \ - 168s^2 - 294s + 5835\right)\eta^2$$

$$\theta = -\frac{\eta}{5}+1+\frac{\Pr}{50}\left(\frac{1}{12}\eta^4-\frac{5}{3}\eta^3+5s\eta^2\right)+\left(-\frac{1}{2}\Pr s+\frac{5}{8}\Pr\eta\right)$$
$$+\frac{\Pr}{30000(\gamma+1)}(-2500\gamma\Pr\eta^3 s-9375\gamma\Pr\eta^2 s+875\gamma\Pr\eta^4 s+7500\Pr\eta^2\gamma s^2)$$
$$+\frac{\Pr}{30000(\gamma+1)}\left(-40\gamma\Pr\eta^5 s-1000\Pr\eta^3\gamma s^2-50M\eta^5\gamma+\frac{50}{3}\gamma\Pr\eta^6\right)$$
$$+\frac{\Pr}{30000(\gamma+1)}\left(-150\eta^5\Pr+100\eta^5\gamma-\frac{3125}{4}\eta^4\gamma+875\eta^4\Pr s\right)$$
$$+\frac{\Pr}{30000(\gamma+1)}\left(125\eta^4\gamma s+7500\Pr s^2\eta^2+\frac{5}{3}M\ \eta^6\gamma-\frac{10}{21}\gamma\Pr\eta^7\right)$$
$$+\frac{\Pr}{30000(\gamma+1)}\left(-40\eta^5\Pr s-10\eta^5\gamma s-1000\Pr s^2\eta^3+\frac{1250}{3}M\eta^4\gamma\right)$$
$$+\frac{\Pr}{30000(\gamma+1)}\left(-2500\eta^3\Pr s-9375\eta^2\Pr s-\frac{625}{4}\Pr\eta^4+3125\Pr\eta^3\right)$$
$$+\frac{\Pr}{30000(\gamma+1)}\left(\frac{50}{3}\eta^6\Pr-\frac{10}{21}\eta^7\Pr+\frac{1}{7}\eta^7\gamma-5\eta^6\gamma\right)$$
$$-\frac{5\Pr\eta}{4032(\gamma+1)}(336\Pr\gamma s^2+700M\gamma-672\Pr\gamma s+336\Pr s^2+255\gamma\Pr) \quad (41)$$
$$-\frac{5\Pr\eta}{4032(\gamma+1)}(-672\Pr s+252s\gamma+255\Pr-1305\gamma)$$

5. RESULTS AND DISCUSSION

HPM of non-linear viscous incompressible hydromagnetic boundary layer flow and heat transfer of a Casson fluid over an exponentially shrinking sheet is studied. The numerical results are presented in graphs. The effects of Casson fluid parameter γ, magnetic interaction parameter M, Prandtl number Pr and suction parameter *s* on velocity, temperature, skin friction and rate of heat transfer are thoroughly analysed.

Figure 2 depicts the velocity profile for various values of Casson fluid parameter γ. This implies that the velocity increase with the increase in the Casson fluid parameter thereby the magnitude of velocity and boundary layer thickness accelerates with an increase in Casson fluid parameter γ. Figure 3 shows the temperature profile for various values of Casson fluid parameter γ. It is noted that the temperature increase with the increase in the Casson fluid parameter. The velocity profile for various values of magnetic parameter *M* is mentioned in Figure 4. It shows that the velocity increase with the increase in the magnetic parameter. Clearly, the momentum boundary layer thickness is enlarged due to increasing values of magnetic parameter *M*.

The temperature profile for various values of magnetic parameter *M* is demonstrated through Figure 5. It shows that the temperature decrease with the increase in the magnetic parameter.

Figure 6 presented the velocity for different profiles for various values of suction parameter *s*. From Figure 6 it is observed that the velocity increase with the increase in the suction parameter. It is noted that a steady raise in the velocity accompanies an arise in the suction parameter.

Figure 7 displays the temperature profile for various values of suction parameters. It is clear that the thermal boundary layer thickness reduces with the larger suction parameter.

Figure 8 portrays the temperature profile for various values of Prandtl number *Pr*. It gives clearly that the temperature decreases with the increase in Prandtl number.

The skin friction coefficient for different values of the magnetic interaction parameter *M* is shown in Figure 9. The skin friction increases with the increase in *M*.

The skin friction coefficient for different values of Casson fluid parameter γ = 1, 5 is presented in Figure 10. It is found that the value of *M* increases with the increase in the value of *M* and the value of γ increase with the increase in the value of γ.

Figure 11 gives the nature of Nusselt number against the Casson fluid parameter with various values of Prandtl number. The increase in the Casson fluid parameter leads to the increase in the Nusselt number.

Figure 12 depicts that the Nusselt number for different values of Prandtl number Pr. It is noted that the effect of Prandtl number Pr decreases the rate of heat transfer whereas the rate of heat transfer increases with increasing Casson fluid parameter.

We compare the applied solution strategies in several stages for $f''(0)$ and $\theta'(0)$. Table 1 show the comparison between Homotopy perturbation method and Runge-Kutta fourth order method for $f''(0)$ in several parameters. Table 2 express the comparison between the applied methods for $\theta'(0)$ in various parameters. According to the provided tables, it is readily realized that the solution strategies are all successful.

Table 1. Comparison between the applied methods for $f''(0)$

			$f''(0)$	$f''(0)$
M	γ	*s*	Homotopy Perturbation Method	Runge-Kutta fourth order Method
1.0 2.0 3.0			0.61033 1.18461 1.47884	0.61031 1.18455 1.47879
	1.0 3.0 5.0		0.61033 1.18869 1.36441	0.61031 1.18866 1.36433
		2.0 2.5 3.0	0.61033 1.00397 1.31021	0.61031 1.00391 1.31012

Table 2. Comparison between the applied methods for $\theta'(0)$

				$\theta'(0)$	$\theta'(0)$
M	γ	s	Pr	Homotopy Perturbation Method	Runge-Kutta fourth order Method
1.0 2.0 3.0				–0.95754 –1.12322 –1.16513	–0.95746 –1.12314 –1.16510
	1.0 3.0 5.0			–0.95754 –1.13083 –1.15711	–0.95746 –1.13078 –1.15702
		2.0 2.5 3.0		–0.95754 –1.50744 –1.93555	–0.95746 –1.50742 –1.93546
			0.5 0.72 1.2	–0.58825 –0.95754 –1.86244	–0.58818 –0.95746 –1.86237

6. CONCLUSION

In this work, the Homotopy Perturbation Method of hydromagnetic flow and heat transfer of a Casson fluid over an exponentially shrinking sheet has been studied. Similarity transformations were introduced to convert the nonlinear partial differential equations into the non-linear ordinary differential equations. Numerical solutions are obtained by using the Homotopy Perturbation Method for several of physical parameters. The effects of different physical parameters governing the flow and heat transfer characteristics on velocity, temperature, skin friction and rate of heat transfer are clearly discussed. Some of the important findings drawn from the investigations are listed as follows.

- The influence of magnetic interaction parameter is to accelerate the velocity and decelerate the temperature distribution.
- Thermal boundary layer thickness decreases with the increasing Prandtl number.
- Effect of Casson fluid parameter is to reduce both the velocity and temperature.
- A comparative study on Homotopy perturbation method and Runge-Kutta fourth order method with shooting technique.

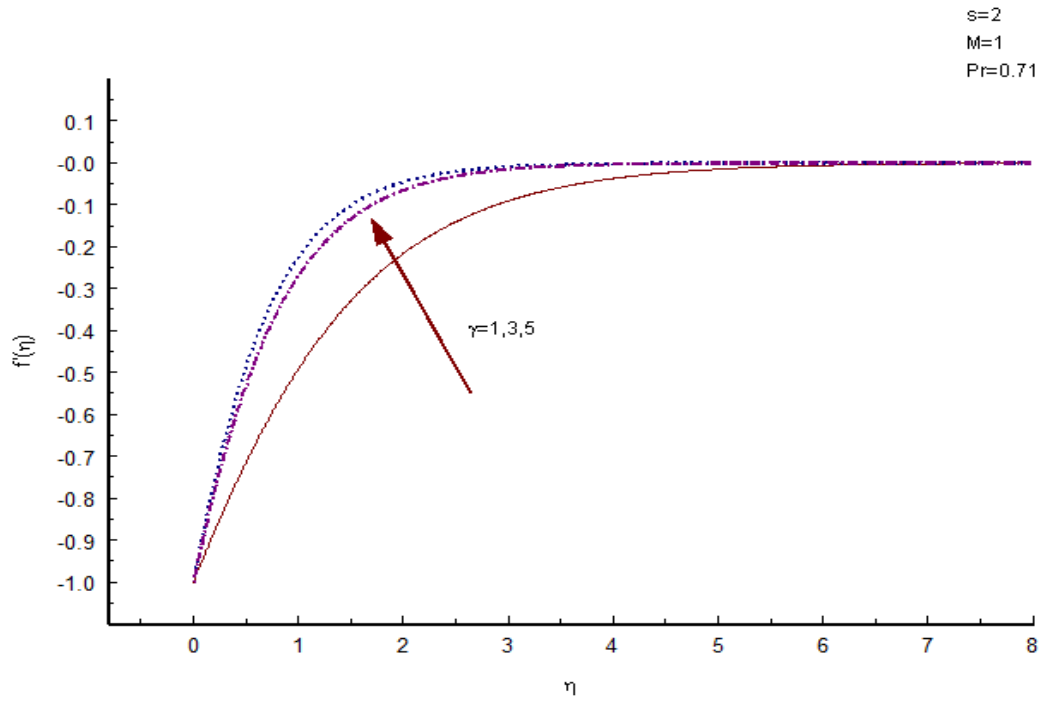

Figure 2. The velocity distribution f'(η) against η for different values of Casson fluid parameter γ

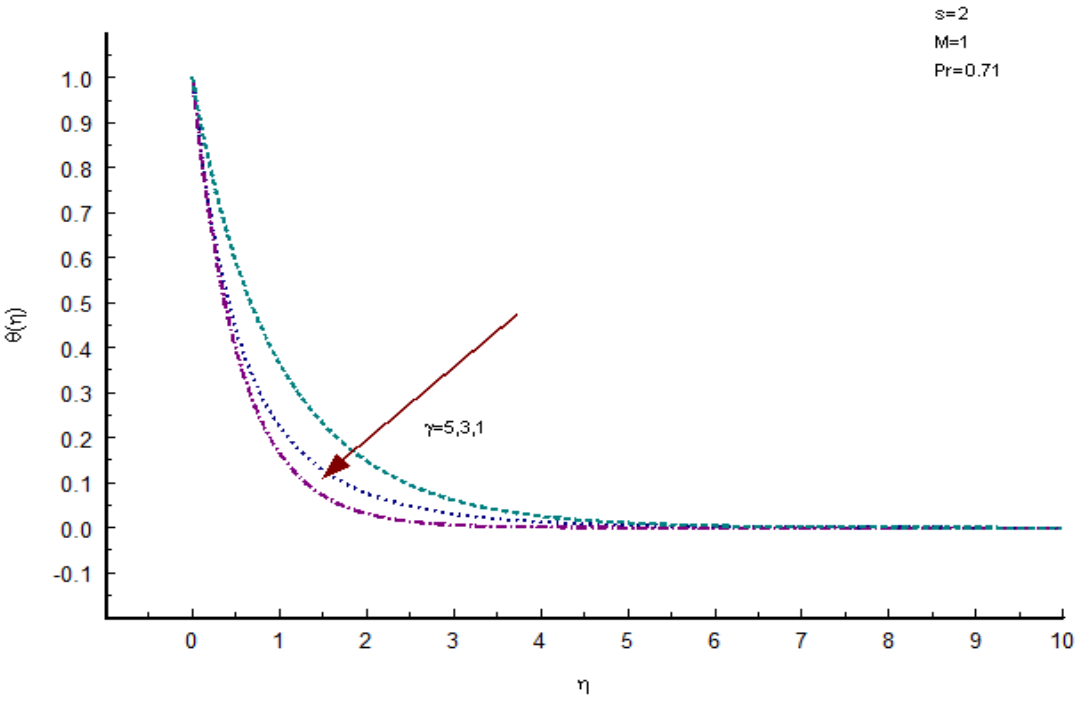

Figure 3. The temperature distribution θ(η) against η for different values of Casson fluid parameter γ

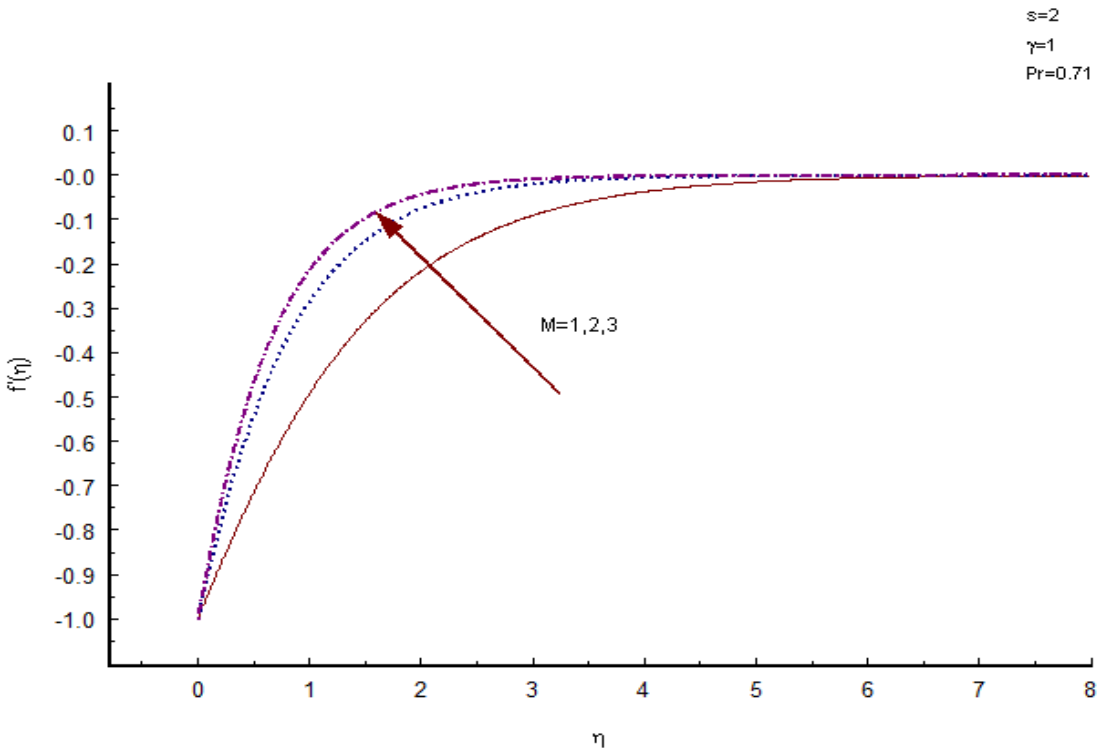

Figure 4. The velocity distribution f'(η) against η for different values of magnetic interaction parameter M

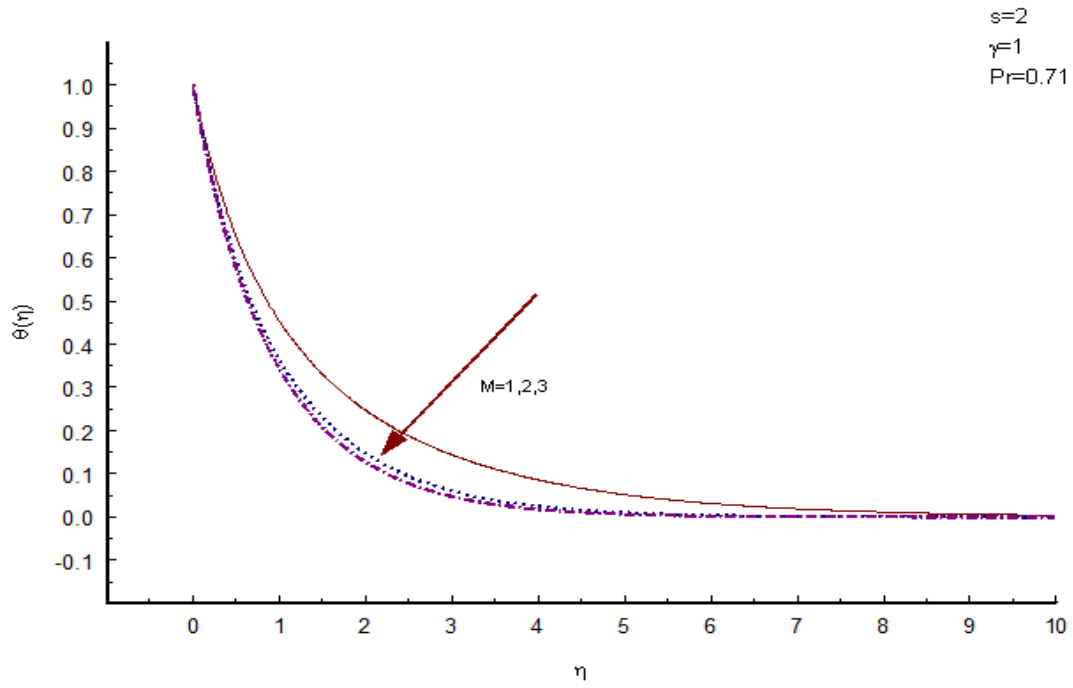

Figure 5. The temperature distribution θ(η) against η for different values of magnetic interaction parameter M

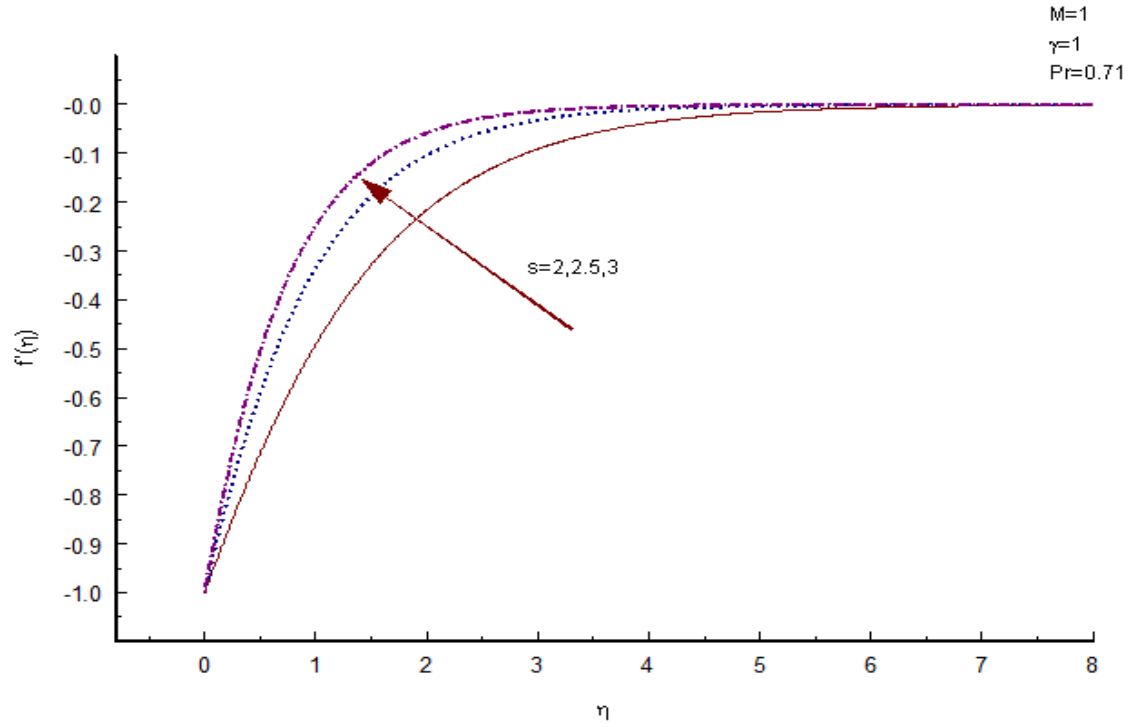

Figure 6. The velocity distribution f'(η) against η for different values of Suction parameter s

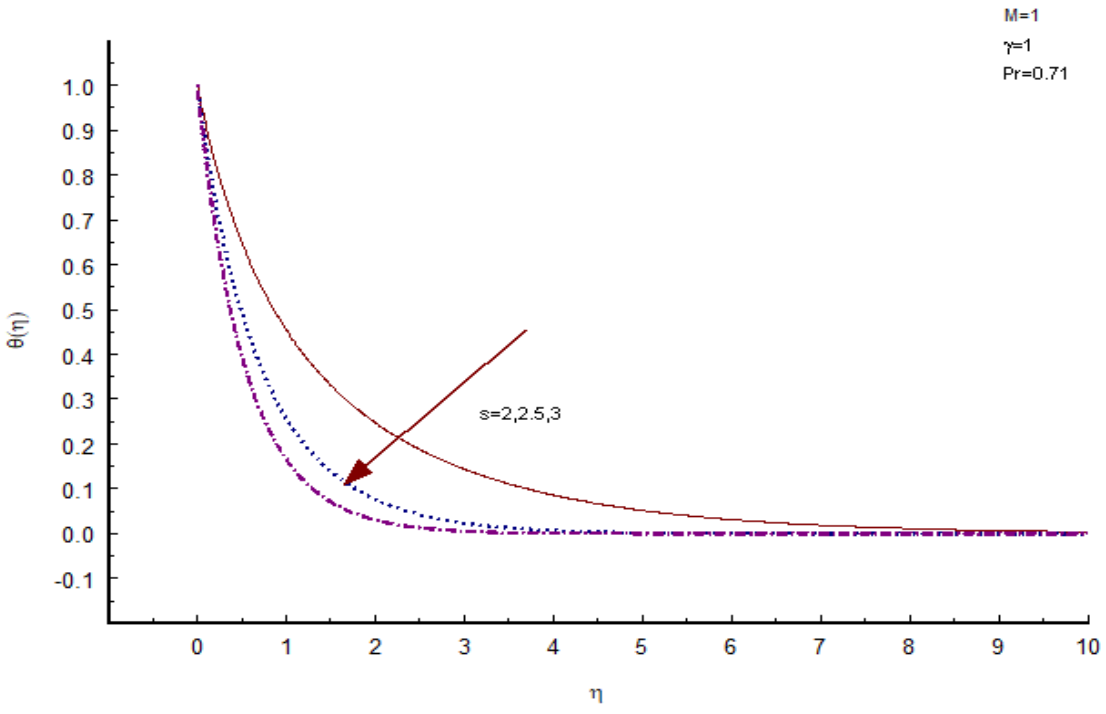

Figure 7. The temperature distribution θ(η) against η for different values of suction parameter s

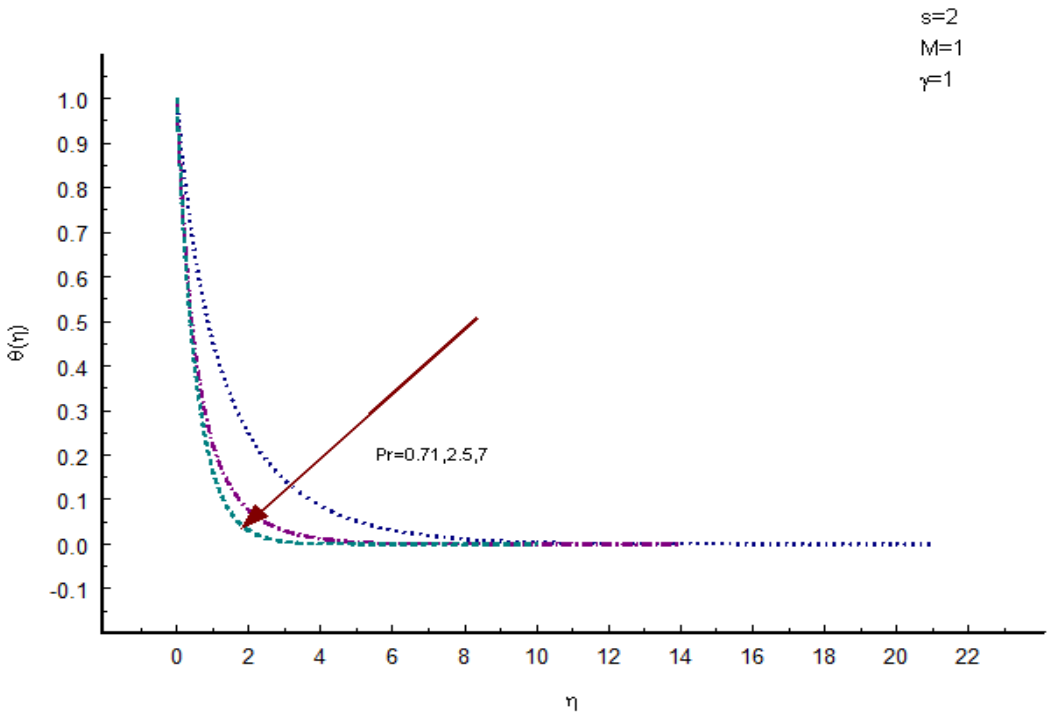

Figure 8. The temperature distribution θ(η) against η for different values of Prandtl number Pr

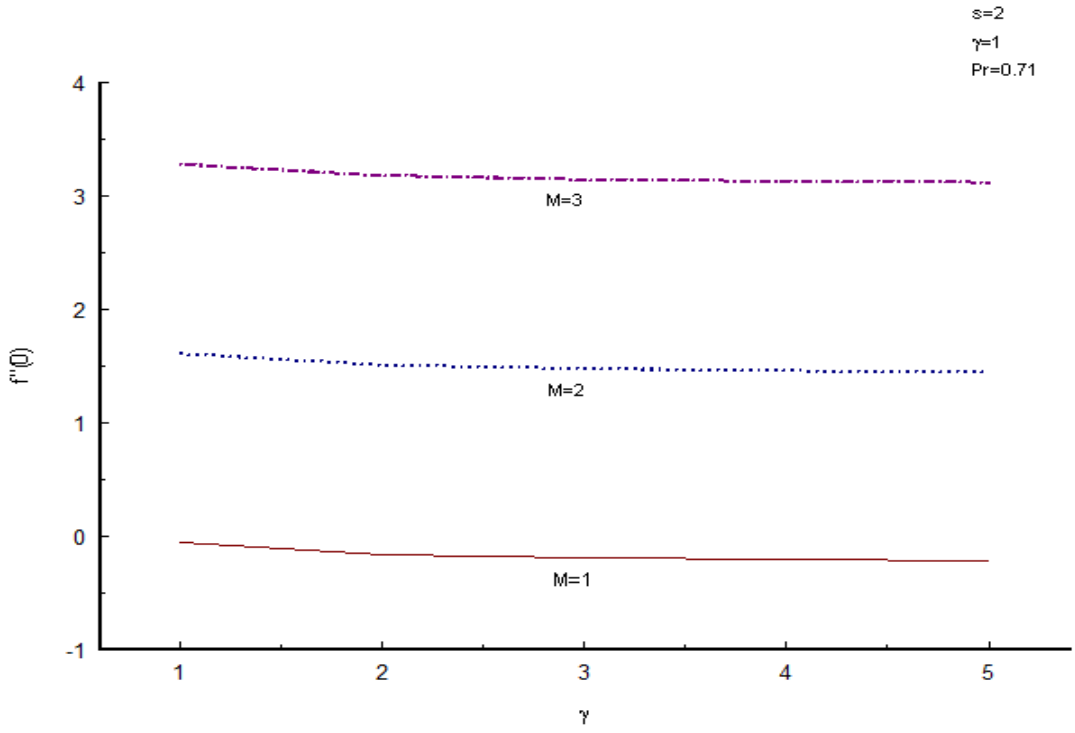

Figure 9. The skin friction against Casson fluid parameter γ for different values of magnetic interaction parameter M

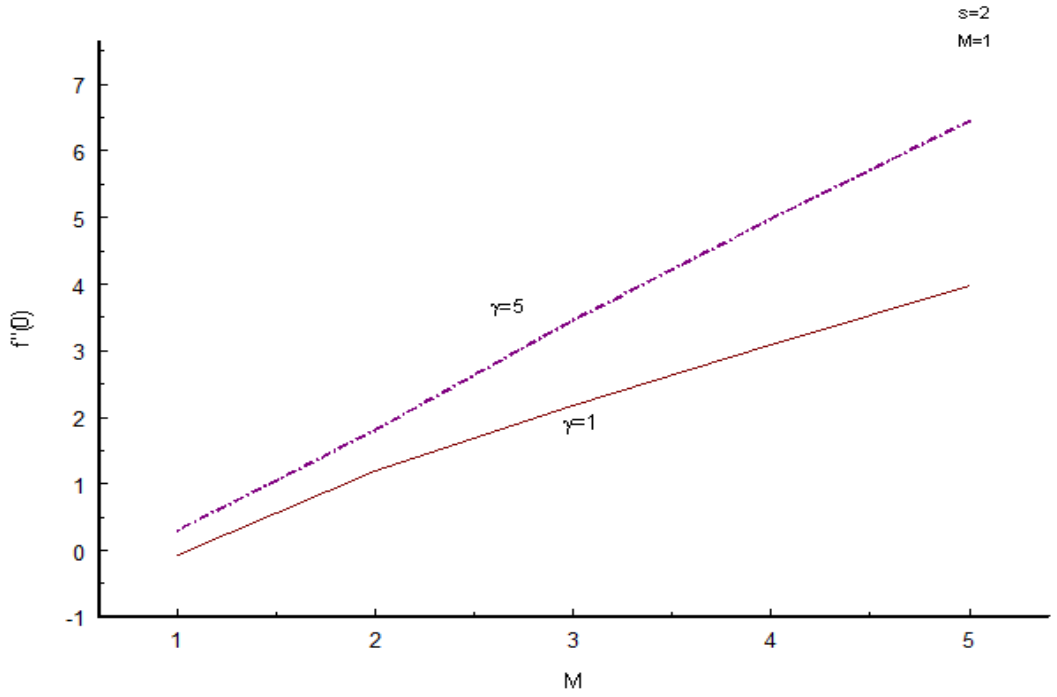

Figure 10. The skin friction against M for different values of Casson fluid parameter γ

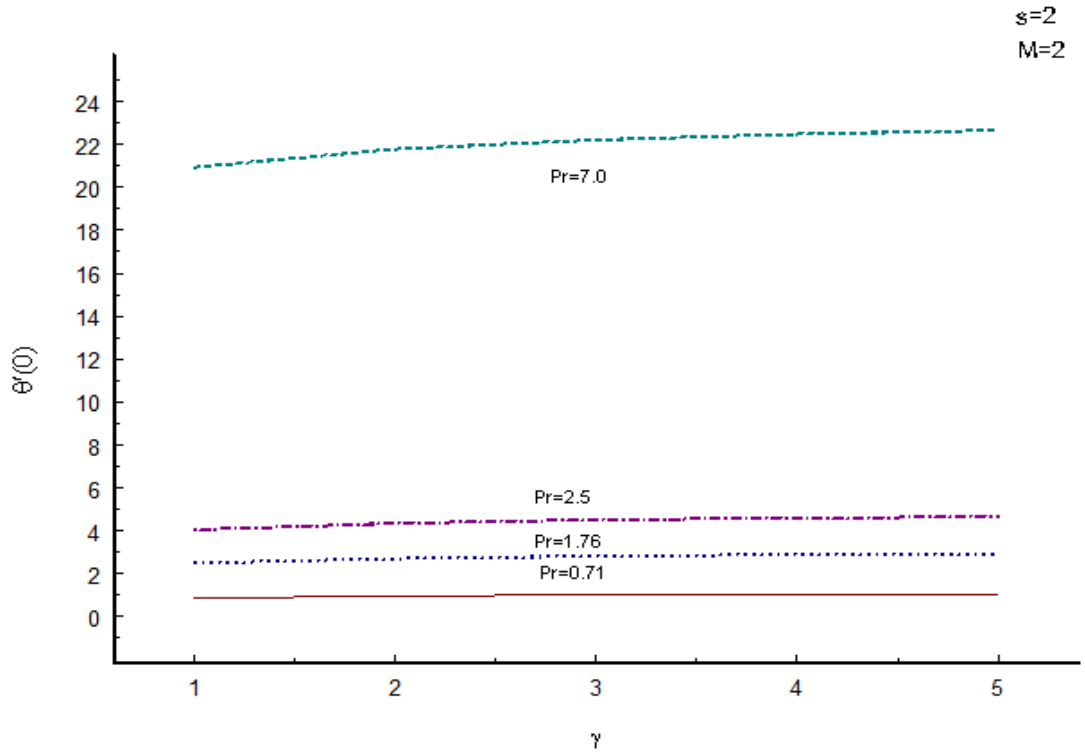

Figure 11. The Nusselt number against Casson fluid parameter γ for different values of Prandtl number Pr when the value of suction parameter s being 2

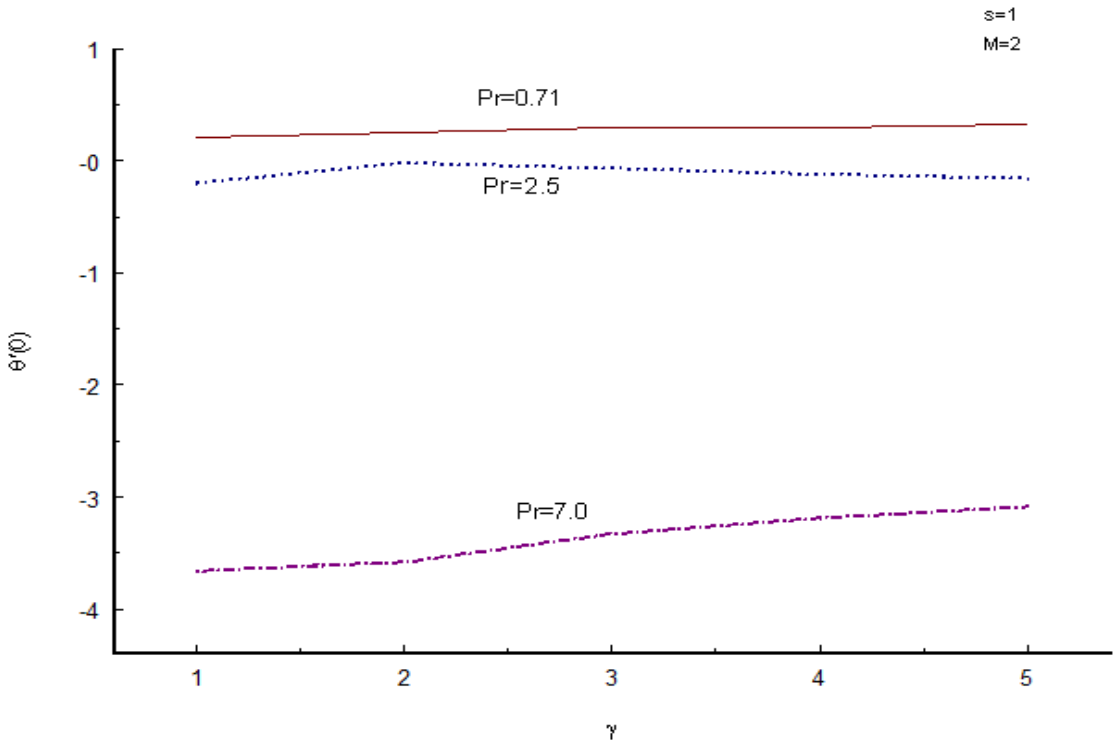

Figure 12. The Nusselt number against Casson fluid parameter γ for different values of Prandtl number Pr when the value of suction parameter s being 1

References

[1] He, J.H. Homotopy Perturbation Technique. *Computer Methods in Applied Mechanics and Engineering*, 178 (1999) 257-262.

[2] Crane, L.J. Flow past a stretching plate, *ZAMP*, 21 (1970) 645-655.

[3] Carragher, P. and Crane, L.J. Heat transfer on continuous stretching sheet. *Z. Angew. Math. Mech.* 62 (1982) 564.

[4] Salem, A.M. and Fathy, R. Effects of variable properties on MHD heat and mass transfer flow near a stagnation point towards a stretching sheet in a porous medium with thermal radiation. *Chin. Phys. Lett. B* 21 (2012) 054701.

[5] Bhattacharyya, K., Mukhopadhyay, S. and Layek, G.C. Slip effects on an unsteady boundary later stagnation-point flow and heat transfer over a stretching sheet. *Chin. Phys. Lett.* 28 (2011) 094702.

[6] Wang, C.Y. Liquid film on an unsteady stretching surface. *Quart. Appl. Math.* 48 (1990) 601-610.

[7] Miklavcic, M. and Wang, C.Y. Viscous flow due to a shrinking sheet. *Quart. Appl. Math.* 64 (2006) 283-290.

[8] Fang, T. and Zhang, J. Closed-form exact solutions of MHD viscous flow over a shrinking sheet. *Commun, Non-linear Sci. Numer. Simul.,* 14 (2009) 2853-2857.

[9] Fang, T., Zhang, J. and Yao, S. Slip Magnetohydrodynamic viscous flow over a Permeable Shrinking sheet. *Chin. Phys. Lett.* 27 (2010) 124702.

[10] Hayat, T. Abbas, Z. Jaued, T. and Sajid, M. Three-dimensional rotating flow induced by a shrinking sheet for suction. *Chaos, Solitons and Fractals* 39 (2009) 1615-1626.

[11] Jhankal, A.K. and Manoj Kumar. MHD Boundary layer flow past over a shrinking sheet with Heat transfer and Mass suction. *International Journal of Computational and Applied Mathematics* 2 (2017) 441-448.

[12] Pramanik, S. Casson fluid flow and heat transfer past an exponentially porous stretching surface in presence of thermal radiation. *Ain Shams Engineering Journal*, 5 (2014) 205-212.

[13] He, J.H. Some asymptotic methods for strongly non-linear equations. *International Journal of Modern Physics* 20 (2006) 1141-1199.

[14] He, J.H. Homotopy Perturbation Method for solving boundary value problems. *Physics Letters A*, 350 (2006) 87-88.

[15] He, J.H. Application of homotopy perturbation method to non-linear wave equations. *Chaos, Solitons and Fractals* 26 (2005) 695-700.

[16] He, J.H. A coupling method of a homotopy technique and a perturbation technique for nonlinear problems. *International Journal of Non-linear Mechanics*, 35 (2000) 37-43.

[17] He, J.H. Homotopy perturbation technique for bifurcation of non-linear problems. *International Journal of Nonlinear Sciences and Numerical Simulation*, 6 (2005) 207-208.

[18] Sadighi, A. and Ganji, D.D. Application of He's homotopy-perturbation method to non-linear coupled systems of reaction-diffusion equations. *International Journal of Non-linear Sciences and Numerical Simulation,* 7(4) (2006) 411-418.

[19] Nourazar, S.S., Habibi Matin, M. and Simiari, M. The HPM Applied to MHD Nanofluid Flow over a Horizontal Stretching Plate. *Journal of Applied Mathematics*, 2011. Volume 2011, Article ID 876437. http://dx.doi.org/10.1155/2011/876437

[20] Thiagarajan, M. and Senthilkumar, K. DTM-Pade Approximants of MHD Boundary-Layer Flow of a Casson Fluid over a Shrinking Sheet. *United States of America Research Journal*, 1(1) (2013) 1-7.

[21] Mustafa, M., Hayat, T., Pop, I. and Hendi, A. Stagnation-point flow and heat transfer of a Casson fluid towards a stretching sheet. *Z. Naturforsch.* 67a (2012) 70-76